 ©ASM International

Physical Processes in Laser-Assisted Aluminum Foaming

Y.P. Kathuria

(Submitted 15 December 2000; in revised form 30 March 2001)

Aluminum foam has become popular in recent years and has the potential to be used in many applications due to its lightweight structure. In this paper, laser-assisted foaming experiments have been performed to fabricate closed cell porous aluminum structures with different relative densities (0.39 to 0.33) and porosities of 61 to 67%. The influence of the processing conditions on the evolution of cell morphology of the foam is investigated. Preliminary results suggest that a pore size gradient and a density gradient exist in the structure as the processing condition changes. The foam has large pores and lower density for slow processing speed, in contrast to the fast processing speed with small pore size but higher density. Additionally, an example of laser-assisted cutting of Al foam is also demonstrated.

Keywords aluminum, foam, laser, microstructure, powder metallurgy

1. Introduction

Recently, there has been growing interest in metal foaming.[1–18] Aluminum foam[2–18] has created a special interest due to its lightweight structure and its various applications in the automotive, aerospace, and allied industries. Besides this, advances in the near net shaping of aluminum foam have expanded its possibilities in structural applications. However, the related manufacturing techniques and characterization methods need greater attention to make their use in industry more effective and economical. Various methods,[2–5] including casting and powder metallurgy techniques, have been used, which employ the conventional melting and molding process to produce the Al foam; however, here, an alternative process of using laser as a heat source will be described. It has an inherent advantage of unidirectional and localized foaming. Besides that, the process is much faster, due to the rapid solidification process, where the stabilization of pore formation can partly be controlled by coaxial gas flow and the laser processing parameters. In the present paper, based upon the powder metallurgy (P/M) and laser heating process, it is demonstrated that this unidirectional and localized expansion of the Al foam using the Nd-YAG/CO_2 laser is feasible. The basic process of beam interaction time with the foamable precursor material is investigated. In addition, an examination is made of the influence of the processing conditions on the evolution of cell morphology, and results concerning the density gradient are interpreted. The combination of such an approach will allow us to study the physical aspects of laser-assisted foaming with respect to its production and quality.

2. Laser-Assisted Foaming

The basic principle of laser-assisted foaming is shown schematically in Fig. 1. It is produced by mixing powdered material and a foaming agent and subsequently cold isostatic pressing the mixture to a foamable sandwich precursor material.[3] The material is foamed by heating it to its melting point by high power laser beam irradiation. The unidirectional expansion of the foamable precursor material can be observed during the entire foaming process in the irradiation direction. The expansion in the other directions is relatively negligibly small. In the aluminum foaming process, first, an aluminum sandwich with Al-foam core is produced. This can be done by mixing the aluminum alloy powder (Al-7% Si) with a fraction of the foaming agent (0.5% TiH_2), its typical particle size being 40 μm. The powder mixture is then compressed to the extrusion billets by a cold isostatic press (CIP), which is about 80% in density. The CIP expandable billets are then extruded between two covering sheets of nonexpandable aluminum to a 100% dense material. During the deformation process under pressure, a metallic bond is created between the material of the covering sheet and the extrusions. The laser irradiation heats this Al-alloy sandwich above its melting point of 660 °C and thereby the binding agent TiH_2 expands the material. It is believed that, at high temperature, the foaming agent titanium hydride decomposes into titanium and hydrogen gas. Titanium released from the foaming agent remains in the aluminum and perhaps precipitates as $TiAl_3$,[6] whereas the hydrogen gas tends to bubble out, causing the melt to expand and to produce foam forming macroscale porosity. However, a fraction of the gas still remains trapped inside the solidified foam, due to its 20-times solubility difference in liquid and solid aluminum, thus accounting for the microscale porosity. The blowing or shield gas Ar, which lends additional help for the formation of the porosity, may also become trapped inside the solidified foam. In the conventional thermal melting process, the average temperature gradient of the interface varies as the bulk temperature is lower. This is accompanied by a slow cooling rate and, hence, a lengthy time for the stabilization of the pores to occur. On the other hand, in the case of the laser process, the average temperature gradient of the interface is much higher, thus providing a faster cooling rate and, hence, pore stabilization. The figure also illustrates as to how the change in processing speed could affect the cell morphology and the expansion ratio of build-up foam.

Y.P. Kathuria, Laser X Co. Ltd., Chiryu-shi Aichi-ken, 472 Japan. Contact e-mail: ypkathuria@aimnet.ne.jp.

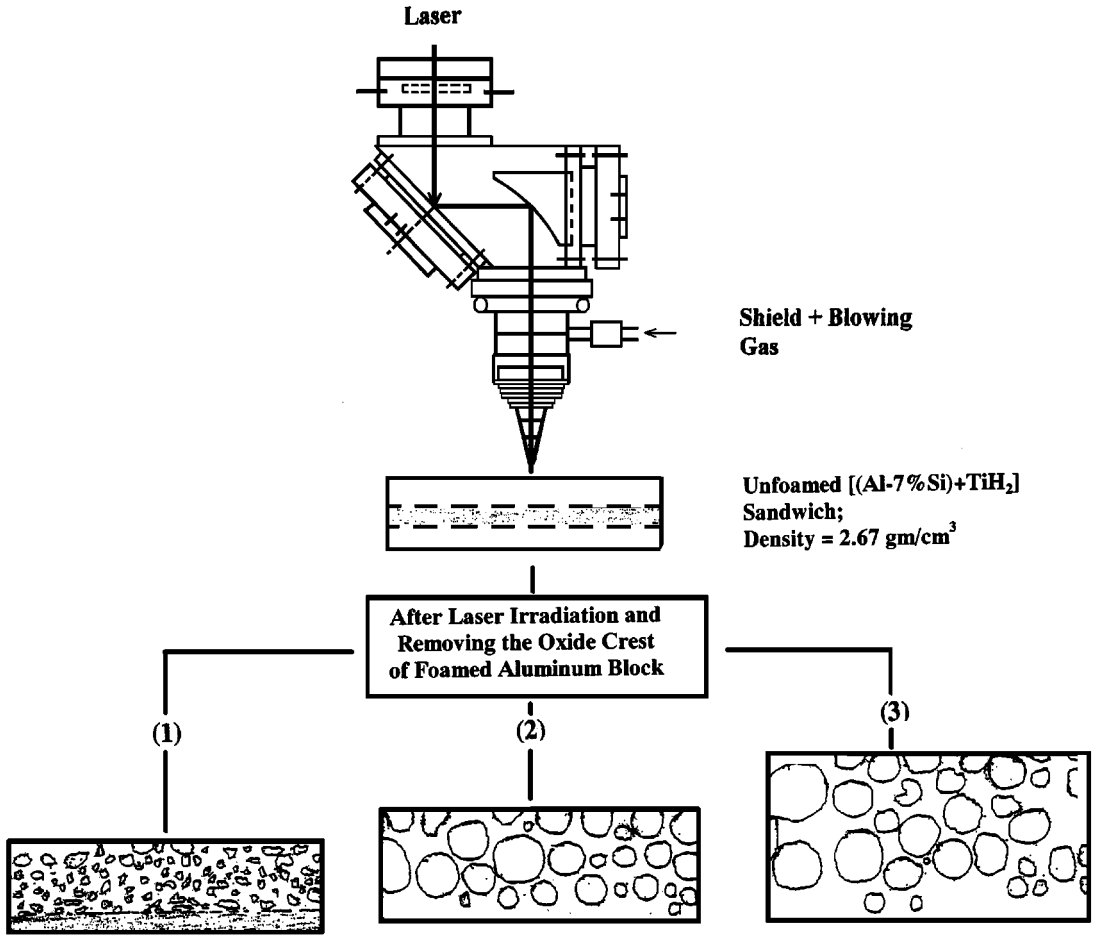

Fig. 1 Block diagram of laser-assisted Al-7% Si foaming for three processing speeds in decreasing order (1) > (2) > (3)

Table 1 Processing parameters

Power (*P*)	3.0–5.0 kW
Spot size	2.0–10.0 mm
Processing speed (*V*)	0.4–2.0 m/min
Ar gas flow rate	20–40 L/min.
Pressure	2.5 kg/cm^2

3. Experimental

The experiments were performed with a 5 kW cw CO_2 laser beam. This is focused further by a 10 in. focal length off-axis parabolic mirror onto the target surface. The working distance was varied to produce a defocused spot size of 2 to 10 mm onto the test piece. An argon gas jet, with a flow rate of 20 to 40 L/min and coaxial to the beam axis, was used to shield the melt pool from oxidation. In the case of foaming, the same gas was also used as the blowing gas. The foamable but unfoamed Al-alloy sandwich sample of size 15 × 15 × 0.4 cm was procured from Fraunhoffer Institute (IFAM) Bremen and fabricated according to the P/M procedure described elsewhere.[2,3] This was further cut into several test pieces of dimensions 50 × 14 × 4 mm, respectively. Due to the fact that they possessed a highly reflective surface, they were made rough by emery paper or by a sand blasting technique and finally black spray coated, to increase the absorption of laser radiation. Foaming was accomplished by irradiating the substrate test piece under the stationary laser beam. The substrate was moved under the beam by the numeric *XY* table. The essential parameters to generate the desired porosities for foamed structure are given in Table 1. To study a different level of porosity, the foaming tracks were made for various processing speeds. A few of the test samples generated with this technique are shown in Fig. 2 to 5, respectively. The measurements of the cell size of the porosity were done microscopically and evaluated[5] as $(ab)^{1/2}$, where *a* and *b* are major and minor axes. For each test sample, 20 point measurements were made at various locations.

The nominal chemical composition of the unfoamed Al-alloy sandwich used is Al-7% Si with approximately 0.5 wt.% TiH_2 as a foaming agent.

In another experiment, as above, a fabricated Al-foam sample of thickness $t = 8.13$ mm was cut with the laser μ jet. It uses a pulsed Nd-YAG laser beam that is guided through a water jet of about 100 μm in diameter. Figure 5(c) also shows an inverted section of such a laser-cut sample. In the conventional cutting of Al foam with the laser, the cut section of the pores is severely damaged due to thermal effects. But when the laser

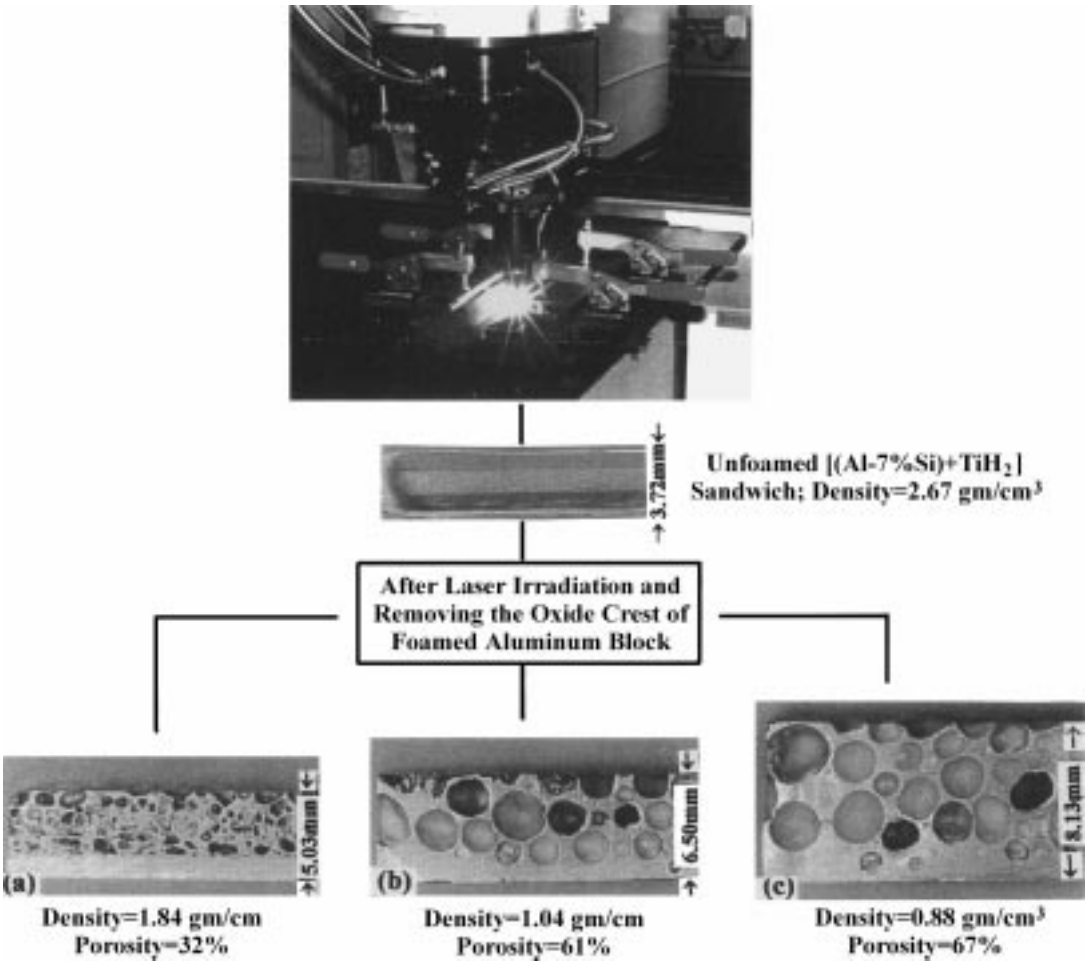

Fig. 2 Laser-assisted Al-7% Si foaming with experimental results. Laser: cw CO_2; P = 5 kW; and Ar = 30 L/min. Processing speed (V) = (**a**) 2 m/min, (**b**) 0.8 m/min, and (**c**) 0.4 m/min

beam is guided through the water jet, the thermal effects are greatly reduced and the cut cross section of the pores, as shown in Fig. 5(c), become relatively better.

4. Results and Discussion

For the microscopic observation of the cell morphology, the top and the side cross section of the foamed Al blocks were made by removing the oxide crest and then polishing with the conventional technique. Figure 2(a) to (c), Fig. 3(a) to (d), and Fig. 4 show the side, edge, and top view sections of the foam, which exhibits a closed cell structure. A strong variation in the cell size or structure can be seen depending upon the processing parameters, and their shape varies from circular to irregular ellipsoidal or deformed circular structure. This variation can be explained by considering the beam interaction time (t_{int} = spot size/processing speed). On careful examination of Fig. 2, one finds that, initially, the width of the unfoamed aluminum sandwich is only 3.72 mm. Upon laser irradiation, it expands predominantly unidirectionally in the direction of the laser beam. The expansion process in the other directions is relatively small and can be neglected. One finds that, at higher processing speeds, there is short beam interaction time (0.16 s), the cell size is relatively fine (≈0.2 mm), and the width of the foamed structure already becomes 5.03 mm (Fig. 2a); however, the base is still not fully expanded. On the other hand, at lower processing speeds, that is, at a long interaction time (0.86 s), the width of the foamed structure is scaled up to 8.13 mm (Fig. 2c), having a large size porosity and a cell size of about 3 mm. Besides that, the cell shape is also partially deformed from its primitive shape due to the gravitational effects on foam, which is playing against the pressure of the blowing agent, which is exerting an internal force on the cells that is equal in all directions.[7]

Furthermore, nonoptimized processing conditions have severe effects on the foaming process. Since TiH_2 absorbs heat when decomposing, the actual melt temperature should be higher than the theoretical temperature.[8] As TiH_2 decomposition starts, the melt temperature drops to the solidification temperature interval. Therefore, if the initial foaming temperature is 660 °C, it will put a restrain on the effective solidification temperature interval for the foaming procedure. Thus, the uniform distribution of the foaming agent is hindered (Fig. 5a).

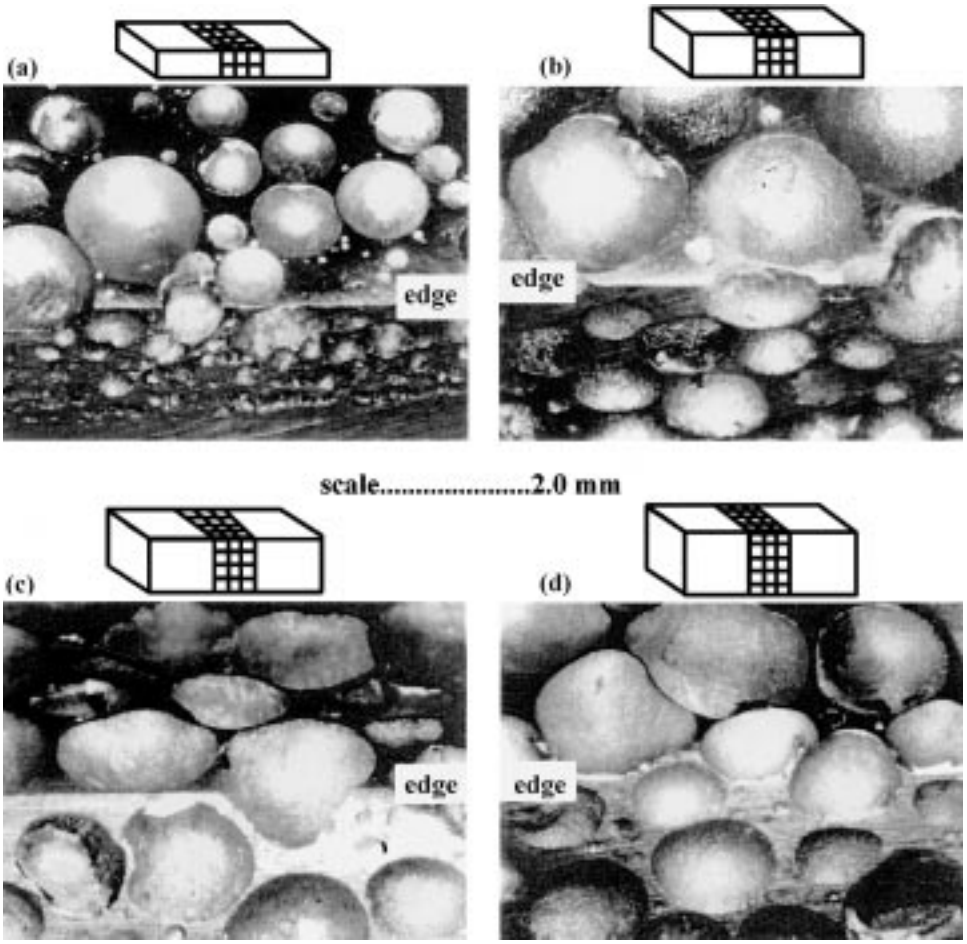

Fig. 3 Pictorial photographic view across the hatched area of Al-7% Si foam: (**a**) $\rho^* = 1.84$ g/cm^3, (**b**) $\rho^* = 1.04$ g/cm^3, (**c**) $\rho^* = 0.93$ g/cm^3, and (**d**) $\rho^* = 0.88$ g/cm^3

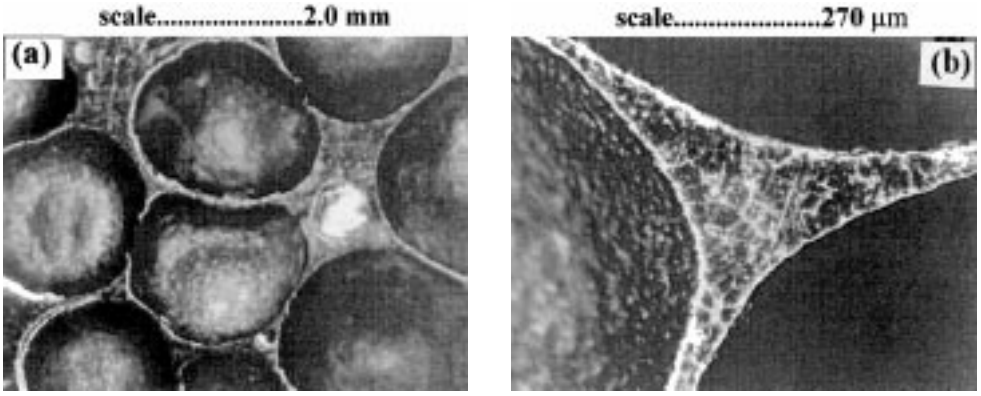

Fig. 4 Optical photographs of the microstructure showing (**a**) pores and (**b**) section between cell walls of Al-7% Si foam

This is especially true in the case of a very fast processing speed, that is, a short interaction time. On the other hand, if the foaming temperature reaches a high value, then the foaming will advance above the temperature level for keeping the alloy as liquid. Because the melt has low viscosity and the bubbles easily aggregate to release, the poor quality of foam is very likely (Fig. 5b). This postcollapse of the pores or foam could be due to the superheat generated when the beam interaction time becomes considerably large.[9] However, at the optimized processing conditions for the foaming temperature, the overall conditions are beneficial to TiH_2 decomposition and the melt foaming that is completed within the solid temperature interval. Microscopically, the cooling rate also varies substantially over the depth of the pool as the temperature gradient is lower at

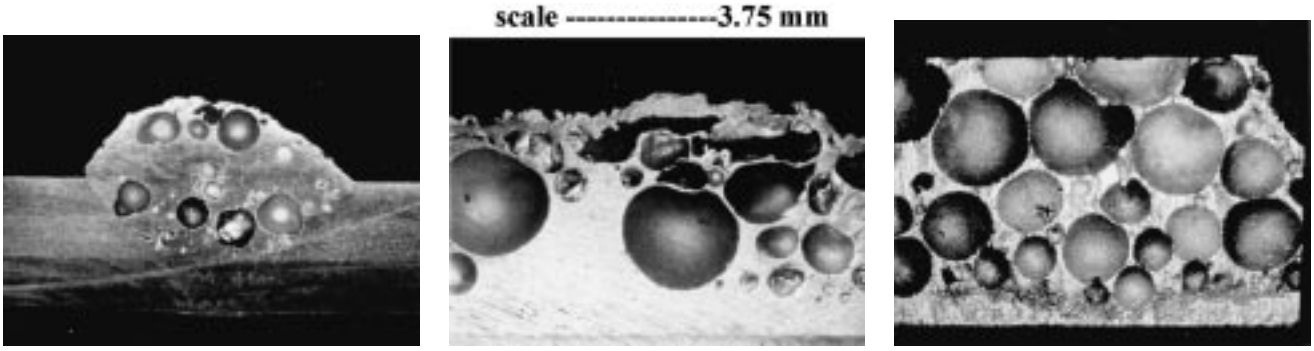

(**a**) (**b**) (**c**)

Fig. 5 Vertical section of Al-7% Si foam for foaming temperature: (**a**) at melting point: underfoaming condition, (**b**) much above melting point: bad quality foam, and (**c**) slightly above melting point: optimum quality foam

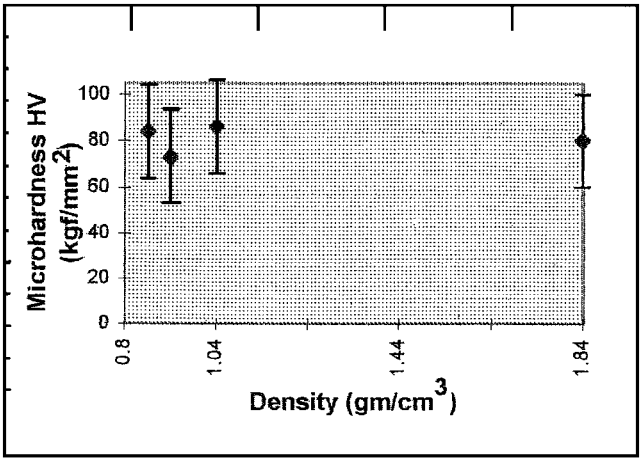

Fig. 6 Microhardness vs density of Al-7% Si foam. Load = 10 gf

Table 2 Density and strain of the Al-7% Si foam

Test sample	(a)	(b)	(c)	(d)
Density (ρ^*) g/cm^3	1.84	1.04	0.93	0.88
Relative Density (ρ^*/ρ_s)	0.68	0.39	0.35	0.33
Porosity [1−(ρ^*/ρ_s)]	32%	61%	65%	67%
Densification Strain [1−1.4(ρ^*/ρ_s)]	0.04	0.46	0.52	0.54
Microhardness (HV)	80	86	73	84

the surface and maximum at the bottom of the pool. Besides that, due to a gradient of the molten liquid pressure, the bubble expands as it moves from the bottom to the top surface. Therefore, one also observes a systematic change in the porosity size from the top to the bottom (Fig. 5c).

For further characterization, the density of each Al-foam block was calculated from the measured weight and the volume. The volume of each foamed specimen was calculated from its dimensions. The densities of these Al-foamed blocks were measured to be ρ^* = 1.84, 1.04, 0.93, and 0.88 g/cm^3. Taking into account the density of the pure aluminum (ρ_s = 2.6989 g/cm^3), various other parameters, for example, relative density, porosity, and densification strain, were calculated[10,11] and are summarized in Table 2. To make an estimate of the cell wall yield strength, microhardness measurements were made on the cell edges, which is at the cross-sectional area between the cells (Fig. 4). A microhardness testing machine from Matsuzawa Co. Ltd., Japan (Model MXT70), fitted with a Vickers' identer and applying a 10 g load was used for all the tests. Figure 6 shows a plot of hardness versus density for the various foamed test samples. The microhardness averaged 81 HV. A rough estimate of the cell wall yield strength was made from this microhardness measurement.[5] This amounts to $\sigma_{ys} \cong$ HV/3, which corresponds to 265 MPa, which is slightly higher than the 250 MPa already reported.[5,12] This is possibly due to higher Si content, and moreover, three points close to the lower limiting value of 0.3 for relative density were considered, in accordance with the above mentioned assumption of yield strength.

5. Conclusions

An experimental study has been carried out to fabricate the laser-assisted aluminum alloy (Al-7% Si) foaming. The main conclusions can be summarized as follows.

- There is a predominantly localized and unidirectional expansion of the foam in the direction of laser irradiation.
- A pore size gradient does exist with the slow and fast processing speeds as well as from the top to bottom of the foamed sample.
- Porous structures with a relative density of 0.33 were created.
- An example of laser-assisted cutting of Al foam was also demonstrated.

References

1. C. Park and S.R. Nutt: *Mater. Sci. Eng.*, 2000, vol. A288, pp. 111-18.

2. G.J. Davies and Shu Zhen: *J. Mater. Sci.*, 1983, vol. 18, pp. 1899-1911.
3. J. Banhart and J. Baumeister: *J. Mater. Sci.*, 1998, vol. 33, pp. 1431-40.
4. C.S. Liu, Z.G. Zhu, F.S. Han, and J. Banhart: *J. Mater. Sci.*, 1998, vol. 33, pp. 1769-75.
5. A.E. Simone and L.J. Gibson: *Acta Mater.*, 1998, vol. 46, pp. 3109-23.
6. Y. Sugimura, J. Meyer, M.Y. He, H. Bartsmith, J. Grenstedt, and A.G. Evans: *Acta Mater.*, 1997, vol. 45, pp. 5245-59.
7. Samuel P. McManus: *Polymer Preprints*, 2000, vol. 41, pp. 1056-57.
8. Shaojun Chu, Quiang Niu, Yixian Lin, and Keng Wu: *Iron Steel Inst. Jpn. Int.*, 2000, vol. 40, pp. 597-600.
9. Y.P. Kathuria: *J. Mater. Sci. Technol.*, 2001, vol. 17, pp. 1-4.
10. *Cellular Solids: Structure and Properties*, 2nd ed., L.J. Gibson and M.F. Ashby, eds., Cambridge University Press, Cambridge, United Kingdom, 1997.
11. K.Y.G. McCullough, N.A. Fleck, and M.F. Ashby: *Acta Mater.*, 1999, vol. 8, pp. 2323-30.
12. E. Andrews, W. Sanders, and L.J. Gibson: Mater. *Sci. Eng.*, 1999, vol. A270, pp. 113-24.
13. P.H. Thornton and C.L. Magee: *Metall. Trans. A*, 1975, vol. 6A, pp. 1253-63.
14. D. Weare and M.A. Fortes: *Adv. Phys.*, 1994, vol. 43, pp. 685-738.
15. T.G. Nieh, J.H. Kinney, and J. Wadsworth: *Scripta Mater.*, 1998, vol. 38, pp. 1487-94.
16. H. Fusheng and Z. Zhengang: *J. Mater. Sci.*, 1999, vol. 31, pp. 291-99.
17. Z.X. Guo, C.S.Y. Jee, N. Oezgueven, and J.R.G. Evans: *J. Mater. Sci. Technol.*, 2000, vol.16, p. 776.
18. C. Koerne, F. Berger, M. Arnold, C. Stadelmann, and R.F. Singer: *J. Mater. Sci. Technol.*, 2000, vol. 16, p. 781.